Manganese overload as a co-factor of neurological symptoms in a patient with sclerosing cholangitis due to Langerhans cell histiocytosis

Langerhans cell histiocytosis (LCH) is a rare myeloid neoplasm characterized by the accumulation of $CD1a^+/CD207^+$ histiocytes within tissue.[1] Diagnosis is based on clinical/radiological presentation coupled with organ infiltration by histiocytes exhibiting Langerhans cell markers (CD1a and CD207) and frequent activation of the mitogen-activating pathway genes (MAP-kinase pathway). The clinical spectrum varies widely, ranging from smoldering disease to life-threatening situations depending on the extent of organ involvement.[1] Notably neurological clinical and radiological signs can occur in about 4-6% of patients (neuro-LCH).[2] The radiological presentation of neuro-LCH includes tumor and pseudo-degenerative patterns. The tumor pattern is characterized by space-occupying lesions with contrast enhancement on T1-weighted magnetic resonance imaging (MRI) and mass effect. In contrast, pseudo-degenerative patterns include atrophy, T2-FLAIR hyperintense white matter abnormalities, and/or spontaneous T1 hyperintense basal ganglia and dentate nuclei. Cerebellar syndrome, pyramidal tract irritation, cognitive changes, and pseudobulbar palsy are the main symptoms of pseudo-degenerative neuro-LCH. Given the lack of specific biomarkers in adults, the accurate diagnosis of pseudo-degenerative neuro-LCH relies heavily on the exclusion of differential diagnoses.

Here we describe manganese-related symptoms in a patient with sclerosing cholangitis complicating LCH, that successfully reversed with an MEK inhibitor. According to French legislation, this case report did not require institutional review board approval and was conducted in accordance with the Declaration of Helsinki.

A 61-year-old woman developed a progressive onset of abdominal pain and jaundice over a 3-month period. Laboratory tests showed elevated liver enzymes (ASAT 372 UI/L, ALAT 621 UI/L, gamma-GT 608 UI/L, alkaline phosphatase 374 UI/L) along with normal bilirubin levels and isolated arginine vasopressin deficiency. Hepatobiliary MRI showed peripheral bile duct dilatation without stenosis of the principal biliary duct compatible with sclerosing cholangitis (Figure 1A), while brain MRI and ^{18}FDG PET-CT were unremarkable (Figure 1B). Liver biopsy showed histiocytic infiltration characteristic of LCH with both *BRAF* c.1457_1471 del, p.(486_490 del) and *DNMT3A* c.1742G>C, p.(Trp5871Ser) mutations (Figure 1C, D). Initially, the patient refused treatment, but due to pruritis secondary to increased bilirubin, she received treatment with vinblastine and steroids.

Results of liver tests worsened (bilirubin: 121 μmol/L; ASAT: 127 UI/L; ALAT: 98 UI/L; Gamma-GT: 43 UI/L, and alkaline phosphatase: 1254 UI/L) and metabolic progression was observed (liver lesion: maximum standardized uptake value [SUV_{max}]: 11.7 *vs*. 8.6 with the onset of 2 liver lesions) after 6 chemotherapy cycles (Figure 1E). Of note, the patient developed gait disturbance leading to falls and fractures at the end of the conventional chemotherapy. Due to the progression of the disease, the patient received targeted therapy with an MEK inhibitor (cobimetinib 20 mg twice a day, 21 days on a 28-day cycle) as the identified deletion causes *in vitro* resistance to BRAF inhibitors but is sensitive to MEK inhibitors. A few days after the initiation of cobimetinib treatment, the patient presented signs of mild extrapyramidal tract with tremors, dysarthric speech, and depressive symptoms. These signs were initially considered to be due to a progression of the patient's neurological disease. She displayed no cerebellar pseudo-bulbar effects or encephalopathy. However, after 2 cycles of cobimetinib, the results of neurological examination remained stable, whereas the patient's jaundice, pruritis, and mild ascites worsened. Liver function worsened, with a total bilirubin concentration of 112 μmol/L (normal levels [N] <12), a direct bilirubin concentration of 86 μmol/L (N<3), and an indirect bilirubin concentration of 26 μmol/L (N<14). Gamma-GT and alkaline phosphatase were 6 times normal levels, whereas ASAT and ALAT were twice normal levels. Prothrombin was 58% (N>70%) with normal factor V (103%) and albumin 24 g/L (N>34). Ferritin was 37 μg/L (range: 8-252) with transferrin at 2.2 g/L (range: 2-3.6). At that time, the patient had cirrhosis with a Child Pugh score of 10-C. Brain MRI showed hyperintense signals of the pallidum, striatum, and substantia nigra with no enhancing T1-weighted (Figure 2A). Cerebrospinal fluid (CSF) analysis showed aseptic meningitis with a moderate elevation of leukocyte levels (13 cells/mm^3, N<10) and normal protein levels. Having ruling out differential diagnoses (e.g., infection, paraneoplastic, or demyelinating syndromes), pseudo-degenerative neuro-LCH was suspected. However, the atypical neurological presentation of neuro-LCH, characterized by extrapyramidal-like features, aseptic meningitis, and T1 basal glia lesions prompted consideration of one remaining differential diagnosis: manganese overload, also historically known as "manganism", which was confirmed by the high concentration of manganese in the blood (58.1 μmol/L, N<15). However, the patient was a secretary by profession and had no known source of manganese intake (enteral nutrition, ephedrine or drugs). No chelation therapy was administered due to the lack of evidence for the efficacy of such treatment in

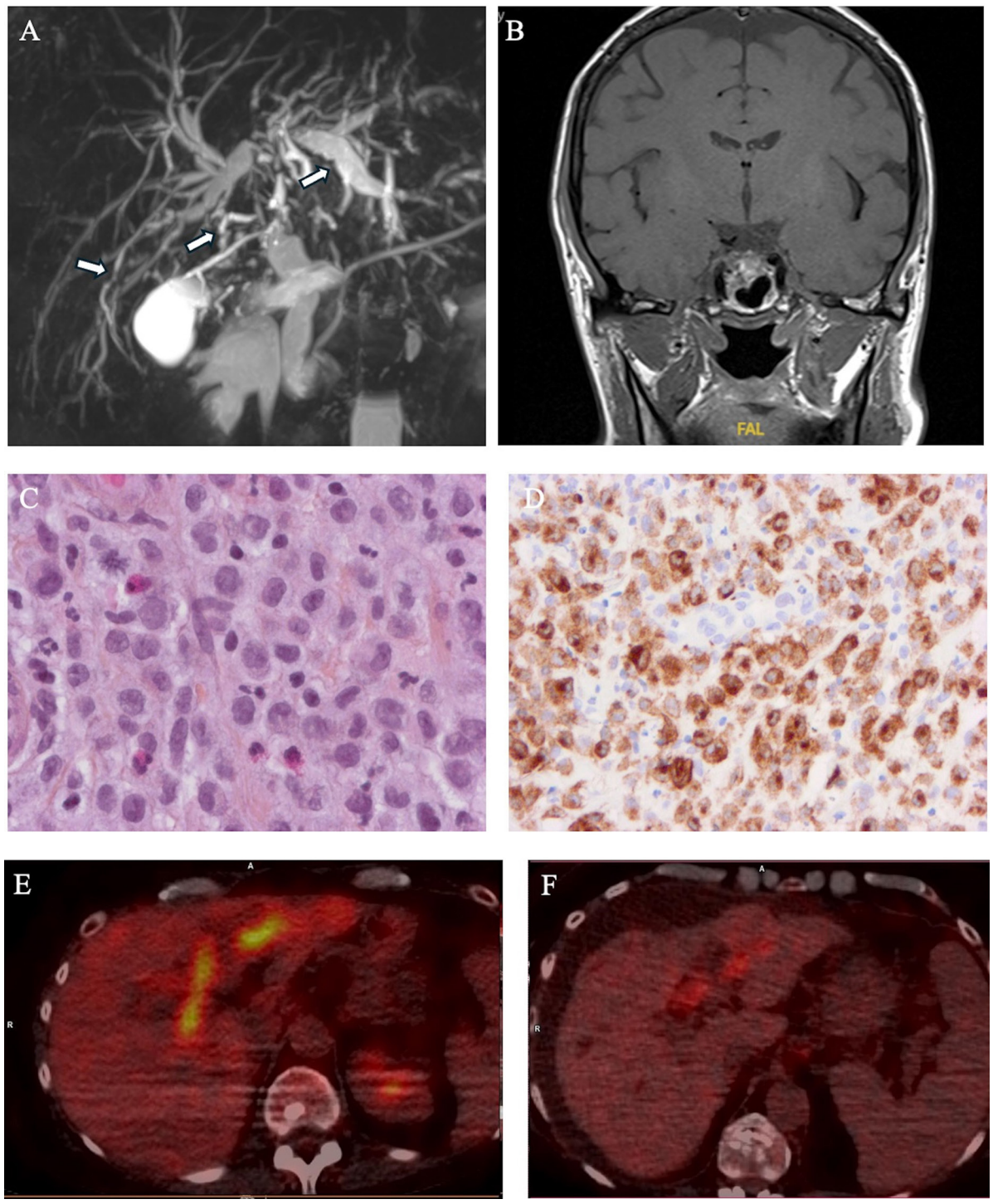

Figure 1. Imaging and pathology features of Langerhans cell histiocytosis. (A) Biliary tract magnetic resonance imaging (MRI) showing peripheral bile duct dilatation, i.e., sclerosing cholangitis, secondary to Langerhans cell histiocytosis (LCH) (white arrows). (B) Normal brain MRI at LCH. (C) Liver biopsy showing portal tract infiltrated by mononucleated histiocytes Hematoxylin&Eosin (H&E) staining. Original magnification ×200. (D) Same sample showing CD207 expression of histiocytes. Original magnification ×200. (E) ^{18}FDG PET showing radiotracer uptake in liver lesions related to LCH evolution at the end of conventional therapy. (F) ^{18}FDG PET showing a decrease in radiotracer uptake after six months of cobimetinib treatment consistent with partial metabolic response.

patients with histiocytosis and concerns about potential hepatic adverse effects.

After six months on cobimetinib therapy, a resolution of the depressive syndrome was observed, accompanied by an improvement in liver function and a partial metabolic response on PET-CT (Figure 1F). Behavioral improvement coincided with a decrease in blood manganese levels to 47 μmol/L and a slight improvement in basal glia lesions on MRI (Figure 2B). Over two years of treatment with cobimetinib, the neurological symptoms, including Parkinson-like features, resolved completely. This resolution was accompanied by further improvement in brain MRI findings (Figure 2C) and a decrease in blood manganese level to 31 μmol/L (Figure 2D), alongside with improvement in liver parameters (ASAT: 1.5N/ALAT:1N; gamma-GT:1N; ALP: 2N; Factor V: 80%; total bilirubin: 88 μmol/L; albumin: 22 g/L) (Table 1). Nonetheless, bili-MRI showed chronic sclerosing cholangitis and the patient experienced cirrhosis-induced complications.

We report here the first description of manganese-induced neurologic features mimicking neurohistiocytosis in an LCH patient with liver involvement. This case highlights the importance of considering all differential diagnoses in patients with suspected neurohistiocytosis.

Manganese is a trace metal that can cause neurological issues in patients with inappropriate exposure.[3] In healthy individuals, blood levels of manganese are very low (4-15 μg/L).[4] Since the discovery of manganism in miners, several factors such as job-related risks,[5] substance abuse,[6] and liver diseases[7] have been associated with manganese overload. Mangansese concentration is tightly regulated by enteral absorption, hepatic metabolism, and biliary excretion.[4] In liver diseases, excess conjugated hyperbilirubinemia and insufficient fecal excretion[8] lead to accumulation within organs, especially in the brain. Neurological symptoms related to manganese exposure are due to brain lesions, particularly affecting basal glia. These symptoms include behavioral changes (e.g., anxiety and depression)

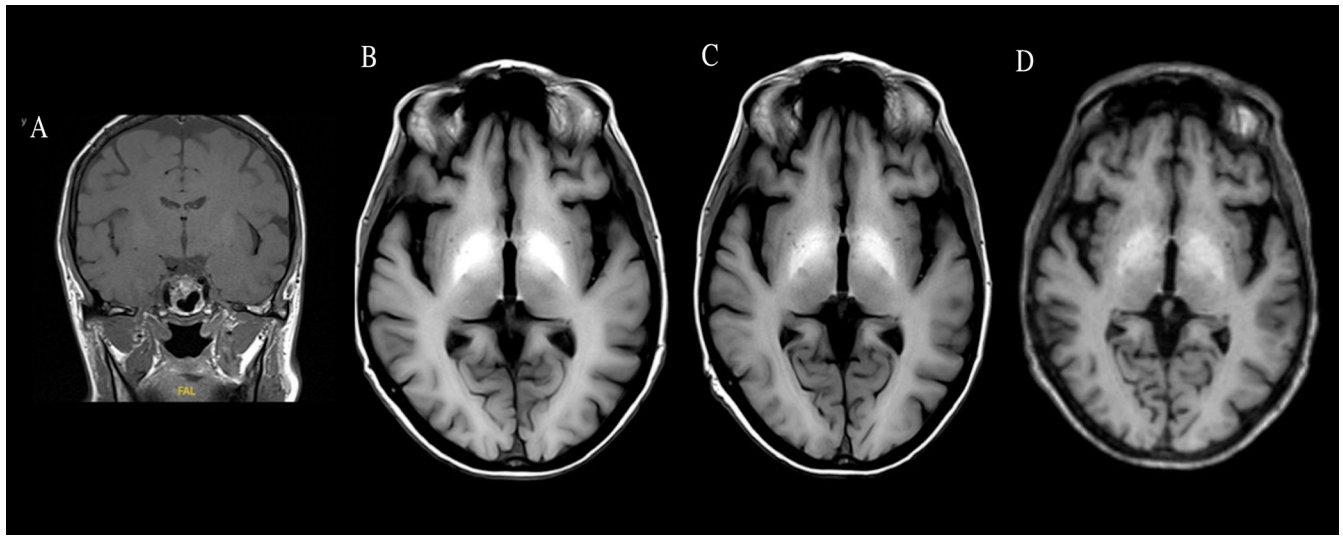

Figure 2. Longitudinal brain magnetic resonance imaging of the patient in T1 sequence. (A) Normal brain magnetic resonance imaging (MRI) at Langerhans cell histiocytosis diagnosis. (B) T1 weighted hyperintense signal in the pallidum at neurological onset (manganese level: 58 μmol/L). (C) Same sequence with a decrease of T1 weighted signal after six months of cobimetinib therapy and decreased blood manganese concentration (47 μmol/L). (D) Same sequence with a decrease in T1 weighted signal after 24 months of cobimetinib therapy and decreased blood manganese concentration (31 μmol/L).

Table 1. Clinical and biological characteristics during the course of Langerhans cell histiocytosis.

	Cobimetinib initiation	Month 6 of cobimetinib treatment	Two years of cobimetinib treatment
Clinical finding	Gait disturbance and fall (responsible for successive both-side femur fracture 2021, 2022, and pelvic fracture 2022) Dysarthric speech Parkinsonism Mild cognitive impairment	- Dysarthric speech Parkinsonism Hepatic encephalopathy triggered by urinary tract infection and esophageal bleeding	Slight improvement of gait disturbance and no falls since cobimetinib initiation - No Parkinsonism -
Biological findings			
Hb, g/dL	11	9.9	9.7
WBC, x10^9/L	5.5	6.5	5
Platelets, x10^9/L	173	154	130
ASAT, UI/L	82	67	93
ALAT, UI/L	63	37	46
Gamma-GT, UI/L	235	85	104
Alkaline phosphatase, UI/L	746	401	398
Total bilirubin, μmol/L	112	140	103
Direct bilirubin, μmol/L	86	113	85
Non-direct bilirubin, μmol/L	26	27	18
Prothrombin time, %	58	36	58
V factor, %	103	56	81
Albumin, g/L	24	21	18
Blood manganese, μmol/L	58.1	47	31
Lumbar puncture	Leukocyte absent Prot 0.09 (g/L) Culture negative	No CSF analysis	Leukocyte absent Prot 0.05 g/L Culture negative
Imaging findings			
Brain MRI	T-1 weighted hyperintensity in the global pallidus, substance nigra and putamen.	No MRI during the encephalopathy	T-1 weighted hyperintensity in the global pallidus, substance nigra and putamen Slight improvement of imaging.
^{18}FDG PET	Progressive disease Liver SUV 11.7	Partial metabolic response SUV 6.8	Partial metabolic response SUV 5.2
Treatment of histiocytosis	Cobimetinib initiation	Cobimetinib	Cobimetinib

CSF: cerebrospinal fluid; Hb: hemoglobin; MRI: magnetic resonance imaging; Prot: protein level; SUV: standardized uptake value; WBC: white blood cell; 18 FDG PET: 18 Fluorodeoxyglucose positron emission tomography.

and Parkinson-like symptoms ranging from tremors or gait disturbances to severe extrapyramidal syndrome. Brain MRI shows non-enhanced T1 hyperintense signals in the pallidum and basal ganglia.[9] Such lesions are not reported in Parkinson's disease.[10] In addition, patients with cirrhosis can develop a similar condition, reported as "acquired hepatocerebral degeneration" due to impaired manganese elimination, in which a liver transplant can slowly restore the neurological condition.

Chelation approaches based on the use of ethylenediaminetetraacetic acid (EDTA) have been proposed in patients with manganese poisoning,[12] but the efficacy of such approaches in other conditions remains uncertain and liver toxicity has been reported.

Neuro-LCH occurs in about 10-20% of patients with tumor, mainly in the skull, or pseudo-degenerative lesions in the posterior fossa.[2] The underlying mechanism of neurodegeneration is complex and secondary to brain invasion by hematopoietic stem cell-derived monocytes or the reactivation of erythro-myeloid progenitors mutated *in utero*.[13,14] Various risk factors, including *BRAF*^{V600E} mutation, pituitary gland infiltration, and skull lesions predispose patients to pseudo-degenerative neuro-LCH,[15] requiring vigilant monitoring and timely intervention. Brain MRI usually highlights T2-FLAIR signal changes in the cerebellar peduncle, medial cerebellar structure, and brainstem,[2] whereas spontaneous hyperintense lesions in the pallidum are rare. Furthermore, the CSF profile is unremarkable[2] and accurate diagnosis is based on the exclusion of differential diagnoses.

In the present case, the behavioral changes combined with Parkinson-like symptoms and aseptic meningitis led us to consider alternative diagnoses, ultimately leading to the detection of manganese accumulation in a patient with sclerosing cholangistis secondary to histiocytosis.

Treatment strategies for LCH vary depending on disease severity and organ involvement.[16] First-line treatment includes a chemotherapy-based regimen (vinblastine or cladribine) for which outcomes are variable, particularly in patients with *BRAF*^{V600E} mutations. Targeted therapies (BRAF or MEK inhibitors) can be proposed for patients with aggressive disease and inadequate response to conventional therapies. In our case, MEK inhibition resulted in a metabolic response alongside with liver improvement.

While the observed neurological improvements may raise questions regarding the underlying etiology (manganese overload or neuro-LCH), the correlation between the late neurological improvement, the amelioration of liver parameters and the decrease in blood manganese levels supports the diagnosis of manganese overload. The long, neurological recovery could be explained by the slower elimination half-life for manganese in the brain than in other organs,[8] reminiscent of the late reversal of acquired hepatocerebral degeneration symptoms with transplant.[17]

This rare presentation needs to be confirmed by further data on manganese assays in histiocytosis with liver involvement showing atypical features for neuro-histiocytosis. Meanwhile, this case emphasizes the importance of considering alternative diagnoses, such as manganese overload, in patients presenting atypical features for neuro-LCH, especially in liver LCH.

Authors

Jerome Razanamahery,[1] Ahmed Idbaih,[2] Matthias Papo,[3] Fabien Robelin,[4] Jean-Francois Emile,[5] Sylvain Audia,[1] Bernard Bonnotte[1#] and Julien Haroche[3#]

[1]Department of Internal Medicine and Clinical Immunology, French Competence Center for Histiocytosis, Dijon University Hospital, Dijon; [2]Sorbonne Université, AP-HP, Institut du Cerveau - Paris Brain Institute - ICM, Inserm, CNRS, Hôpitaux Universitaires La Pitié Salpêtrière - Charles Foix, DMU Neurosciences, Service de Neuro-Oncologie-Institut de Neurologie, F-75013, Paris; [3]Sorbonne University, Internal Medicine Department 2, Institut E3M, French Reference Centre for Histiocytosis, Pitié-Salpêtrière, Paris; [4]Department of Neuroradiology, Dijon University Hospital, Dijon and [5]Department of Pathology, Ambroise Pare Hospital, Paris, France

[#]BB and JH contributed equally as senior authors.

Correspondence:
J. RAZANAMAHERY - jerome.razanamahery@chu-dijon.fr

https://doi.org/10.3324/haematol.2024.286366

Received: July 30, 2024.
Accepted: January 8, 2025.
Early view: January 16, 2025.

Disclosures

No conflicts of interest to disclose.

Contributions

JR was in charge of the patient, collected the data and wrote the initial draft. JH, MP, SA and BB were in charge of the patient. AI provided clinical expertise. FR provided the imaging. JFE confirmed the histological diagnosis and performed the molecular analysis. All authors critically reviewed the manuscript and approved the final draft.

Data-sharing statement

Complete data, including the manganese dosage procedure, can be requested from the corresponding author.

References

1. Allen CE, Merad M, McClain KL. Langerhans-cell histiocytosis. N Engl J Med. 2018;379(9):856-868.
2. Cohen Aubart F, Idbaih A, Emile J-F, et al. Histiocytosis and the nervous system: from diagnosis to targeted therapies. Neuro Oncol. 2021;23(9):1433-1446.
3. Budinger D, Barral S, Soo AKS, Kurian MA. The role of manganese dysregulation in neurological disease: emerging evidence. Lancet Neurol. 2021;20(11):956-968.
4. Williams M, Todd GD, Roney N, et al. Toxicological profile for manganese [Internet]. Atlanta (GA): Agency for Toxic Substances and Disease Registry (US); 2012. http://www.ncbi.nlm.nih.gov/books/NBK158872/ Accessed Apr 15, 2024.
5. Criswell SR, Nielsen SS, Warden MN, et al. MRI signal intensity and Parkinsonism in manganese-exposed workers. J Occup Environ Med. 2019;61(8):641-645.
6. Sikk K, Taba P. Methcathinone “kitchen chemistry” and permanent neurological damage. Int Rev Neurobiol. 2015;120:257-271.
7. Shin H-W, Park HK. Recent updates on acquired hepatocerebral degeneration. Tremor Other Hyperkinet Mov (N Y). 2017;7:463.
8. O’Neal SL, Zheng W. Manganese toxicity upon overexposure: a decade in review. Curr Environ Health Rep. 2015;2(3):315-328.
9. Avelino MA, Fusão EF, Pedroso JL, et al. Inherited manganism: the “cock-walk” gait and typical neuroimaging features. J Neurol Sci. 2014;341(1-2):150-152.
10. Bloem BR, Okun MS, Klein C. Parkinson’s disease. Lancet. 2021;397(10291):2284-2303.
11. Rajoriya N, Brahmania M, Feld J. Implications of manganese in chronic acquired hepatocerebral degeneration. Ann Hepatol. 2019;18(1):274-278.
12. Blanusa M, Varnai VM, Piasek M, Kostial K. Chelators as antidotes of metal toxicity: therapeutic and experimental aspects. Curr Med Chem. 2005;12(23):2771-2794.
13. Mass E, Jacome-Galarza CE, Blank T, et al. A somatic mutation in erythro-myeloid progenitors causes neurodegenerative disease. Nature. 2017;549(7672):389-393.
14. Wilk CM, Cathomas F, Török O, et al. Circulating senescent myeloid cells infiltrate the brain and cause neurodegeneration in histiocytic disorders. Immunity. 2023;56(12):2790-2802.e6.
15. Héritier S, Barkaoui M-A, Miron J, et al. Incidence and risk factors for clinical neurodegenerative Langerhans cell histiocytosis: a longitudinal cohort study. Br J Haematol. 2018;183(4):608-617.
16. Goyal G, Tazi A, Go RS, et al. Expert consensus recommendations for the diagnosis and treatment of Langerhans cell histiocytosis in adults. Blood. 2022;139(17):2601-2621.
17. Qavi AH, Hammad S, Rana AI, et al. Reversal of acquired hepatocerebral degeneration with living donor liver transplantation. Liver Transpl. 2016;22(1):125-129.